JOURNAL OF MATERIALS SCIENCE 29 (1994) 141–150

A generalized law of mixtures

Z. FAN, P. TSAKIROPOULOS, A. P. MIODOWNIK
Department of Materials Science and Engineering, The University of Surrey, Guildford, Surrey GU2 5XH, UK

The mechanical properties of two-phase composites are predicted using a rigorous continuum mechanics analysis and an equivalent microstructural transformation approach. This leads to a generalized law of mixtures which is contrasted with the classical linear law of mixtures which requires some explicit assumptions. The generalized law of mixtures enables prediction of a variety of mechanical properties of a two-phase composite with any volume fraction, grain shape and phase distribution. It is shown that the classical linear law of mixtures is a specific case of the generalized law of mixtures. Examples are given from continuous Cu–W composites, the particulate Co–WC system, Al/SiC_p composites, α–β Ti–Mn alloys and α–β Cu–Zn alloys for the predictions of properties such as Young's modulus, yield strengths, flow stresses, the overall friction stresses and the overall Hall–Petch coefficients. It is shown that the theoretical predictions by the generalized law of mixtures are in very good agreement with the corresponding experimental results drawn from the literature, for both continuous fibre composites and particulate reinforced systems.

1. Introduction

The term "law of mixtures" refers normally to the expression of the mechanical properties of a phase mixture in terms of the bulk or *in situ* mechanical properties and the relative amounts of its constituent phases. In other words, the mechanical properties of a phase mixture are expressed in terms of the relative contributions of the constituent phases.

The law of mixtures was first proposed by Voight [1] to predict the mechanical properties of a composite in terms of the bulk mechanical properties of its constituent phases. This form of the law of mixtures is often called the classical linear law of mixtures. The latter has the following forms for the flow stress and the total strain of a composite containing two-phases, α and β

$$\sigma_f^c = \sigma_f^\alpha f_\alpha + \sigma_f^\beta f_\beta \quad (1a)$$

$$\varepsilon_T^c = \varepsilon_T^\alpha f_\alpha + \varepsilon_T^\beta f_\beta \quad (1b)$$

where σ_f^α, σ_f^β and σ_f^c are the flow stresses of bulk α-alloy, bulk β-alloy and the α–β phase mixture, respectively, ε_T^α, ε_T^β and ε_T^c are the total strains in bulk α-alloy, bulk β-alloy and the α–β phase mixture, respectively, and f is the volume fraction. Equation 1a is called the equal strain model from the assumption that both phases have the same total strain during the deformation process. Equation 1b is called the equal stress model because equal stress is assumed for both phases. The classical linear law of mixtures assumes implicitly that there is no interaction between two constituent phases. However, these assumptions are too simplistic, and moreover, the flow properties of most particulate two-phase composites do not follow this linear law of mixtures.

A more general but still empirical law of mixtures relating to the average stresses and strains in each phase was suggested by Tamura *et al.* [2]. For a composite consisting of two phases, α and β, under uniaxial loading, the stress and strain can be expressed by the following equations

$$\sigma_f^c = \bar{\sigma}_f^\alpha f_\alpha + \bar{\sigma}_f^\beta f_\beta \quad (2a)$$

$$\varepsilon_T^c = \bar{\varepsilon}_T^\alpha f_\alpha + \bar{\varepsilon}_T^\beta f_\beta \quad (2b)$$

where $\bar{\sigma}$ and $\bar{\varepsilon}$ are the average values, respectively, of the directional components of stress and strain parallel to the loading direction of the applied stress averaged on the planes normal to the loading direction for stress or along the lines parallel to the loading direction for strain [3]. Equation 2a and b have been called the modified law of mixtures, because the relevant average stresses and strains of each phase are *in situ* values. In the modified law of mixtures, the interaction effects are incorporated into the stress and strain values associated with each phase. The empirical use of the modified law of mixtures for stress and/or strain has shown good agreement with experiments [3–6], modelling [7–9] and finite element analysis [10, 11]. However, it has been shown recently by Gurland and Cho [12, 13] that the modified law of mixtures can be justified only at small strains.

In this paper, a generalized law of mixtures is developed for the prediction of various mechanical properties of two-phase composites with any volume fraction, grain shape and phase distribution. The generalized law of mixtures is then applied to two-phase composites to predict their mechanical properties. The predictions are verified by the experimental results in the corresponding composite systems.

0022–2461

2. Microstructural characterization

Gurland [14] proposed in 1958 the topological parameter, contiguity (denoted C), for the description of the extent of particle contact in dual-phase structures. Lee and Gurland [9] defined in 1978 the concept of continuous volume and derived the mathematical expression for it in terms of the contiguity and volume fraction. Based on these works, Fan [15] proposed the concepts of separation (denoted S), separated volume, degree of continuity and degree of separation. The definitions, expressions for measurements and calculations under the assumption of random distribution of equiaxed grains are summarized in Table I. The combination of such topological parameters can offer a full description of the phase distribution in the dual-phase structure. All these parameters can be measured experimentally in a microstructure with any grain size, grain shape and phase distribution using standard metallographic methods [16], but they can only be mathematically calculated from the known grain size and volume fraction under the assumption of equiaxed grain and random distribution.

According to the topological transformation [15, 17], a dual-phase microstructure with any grain size, grain shape and phase distribution, as schematically illustrated in Fig. 1a, can be topologically transformed into a three-microstructural-element body (the 3-E body), which is schematically illustrated in Fig. 1b. Element I (EI) consists only of α-grains with an average grain size of d_α and therefore contains only α-grain boundaries. The volume fraction of EI is defined by the continuous volume of α-phase $f_{\alpha c}$; Element II (EII) consists only of β-grains with an average grain size of d_β, and with a volume fraction of $f_{\beta c}$. Only β-grain boundaries exist in EII; Element III (EIII) consists of the long-range α–β chains, hence, there are

TABLE I Summary of the topological parameters (from 15)

Parameter	Definition	Measurement	Calculation
C_α	$C_\alpha = \dfrac{2S_V^{\alpha\alpha}}{2S_V^{\alpha\alpha} + S_V^{\alpha\beta}}$	$C_\alpha = \dfrac{2N_L^{\alpha\alpha}}{2N_L^{\alpha\alpha} + N_L^{\alpha\beta}}$	$C_\alpha = \dfrac{f_\alpha d_\beta}{f_\alpha d_\beta + f_\beta d_\alpha} = \dfrac{f_\alpha R}{f_\alpha R + f_\beta}$
C_β	$C_\beta = \dfrac{2S_V^{\beta\beta}}{2S_V^{\beta\beta} + S_V^{\alpha\beta}}$	$C_\beta = \dfrac{2N_L^{\beta\beta}}{2N_L^{\beta\beta} + N_L^{\alpha\beta}}$	$C_\beta = \dfrac{f_\beta d_\alpha}{f_\alpha d_\beta + f_\beta d_\alpha} = \dfrac{f_\beta}{f_\alpha R + f_\beta}$
S_α	$S_\alpha = \dfrac{S_V^{\alpha\beta}}{2S_V^{\alpha\alpha} + S_V^{\alpha\beta}}$	$S_\alpha = \dfrac{N_L^{\alpha\beta}}{2N_L^{\alpha\alpha} + N_L^{\alpha\beta}}$	$S_\alpha = \dfrac{f_\beta d_\alpha}{f_\alpha d_\beta + f_\beta d_\alpha} = \dfrac{f_\beta}{f_\alpha R + f_\beta}$
S_β	$S_\beta = \dfrac{S_V^{\alpha\beta}}{2S_V^{\beta\beta} + S_V^{\alpha\beta}}$	$S_\beta = \dfrac{N_L^{\alpha\beta}}{2N_L^{\beta\beta} + N_L^{\alpha\beta}}$	$S_\beta = \dfrac{f_\alpha d_\beta}{f_\alpha d_\beta + f_\beta d_\alpha} = \dfrac{f_\alpha R}{f_\alpha R + f_\beta}$
$f_{\alpha c}$	$f_{\alpha c} = \dfrac{\Sigma V_{i\alpha}^{\alpha\alpha}}{V}$	$f_{\alpha c} = C_\alpha f_\alpha$	$f_{\alpha c} = \dfrac{f_\alpha^2 d_\beta}{f_\alpha d_\beta + f_\beta d_\alpha} = \dfrac{f_\alpha^2 R}{f_\alpha R + f_\beta}$
$f_{\beta c}$	$f_{\beta c} = \dfrac{\Sigma V_{i\beta}^{\beta\beta}}{V}$	$f_{\beta c} = C_\beta f_\beta$	$f_{\beta c} = \dfrac{f_\beta^2 d_\alpha}{f_\alpha d_\beta + f_\beta d_\alpha} = \dfrac{f_\beta^2}{f_\alpha R + f_\beta}$
$f_{\alpha s}$	$f_{\alpha s} = \dfrac{\Sigma V_{i\alpha}^{\alpha\beta}}{V}$	$f_{\alpha s} = S_\alpha f_\alpha$	$f_{\alpha s} = \dfrac{f_\alpha f_\beta d_\alpha}{f_\alpha d_\beta + f_\beta d_\alpha} = \dfrac{f_\alpha f_\beta R}{f_\alpha R + f_\beta}$
$f_{\beta s}$	$f_{\beta s} = \dfrac{\Sigma V_{i\beta}^{\alpha\beta}}{V}$	$f_{\beta s} = S_\beta f_\beta$	$f_{\beta s} = \dfrac{f_\alpha f_\beta d_\beta}{f_\alpha d_\beta + f_\beta d_\alpha} = \dfrac{f_\alpha f_\beta}{f_\alpha R + f_\beta}$
F_c	$F_c = f_{\alpha c} + f_{\beta c}$	$F_c = C_\alpha f_\alpha + C_\beta f_\beta$	$F_c = \dfrac{f_\alpha^2 d_\beta + f_\beta^2 d_\alpha}{f_\alpha d_\beta + f_\beta d_\alpha} = \dfrac{f_\alpha^2 R + f_\beta^2}{f_\alpha R + f_\beta}$
F_s	$F_s = f_{\alpha s} + f_{\beta s}$	$F_s = S_\alpha f_\alpha + S_\beta f_\beta$	$F_s = \dfrac{f_\alpha f_\beta (d_\alpha + d_\beta)}{f_\alpha d_\beta + f_\beta d_\alpha} = \dfrac{f_\alpha f_\beta (1 + R)}{f_\alpha R + f_\beta}$

Notes:
d_α, d_β: grain size of α-phase and β-phase
f_α, f_β: volume fraction of α-phase and β-phase
C_α, C_β: contiguity of α-phase and β-phase
S_α, S_β: separation of α-phase and β-phase
$f_{\alpha c}$, $f_{\beta c}$: continuous volume fractions of α-phase and β-phase
$f_{\alpha s}$, $f_{\beta s}$: separated volume fraction of α-phase and β-phase
F_c: degree of continuity of an α–β phase mixture
F_s: degree of separation of an α–β phase mixture
$S_V^{\alpha\alpha}$: surface area between α-grains per unit volume
$S_V^{\beta\beta}$: surface area between β-grains per unit volume
$S_V^{\alpha\beta}$: surface area between α- and β-grains per unit volume
$S_V^\alpha = S_V^{\alpha\alpha} + 2S_V^{\alpha\beta}$: total α-grain boundary area per unit volume
$S_V^\beta = S_V^{\beta\beta} + 2S_V^{\alpha\beta}$: total β-grain boundary area per unit volume
$N_L^{\alpha\alpha}$ and $N_L^{\beta\beta}$: numbers of intercepts of α–α interfaces and β–β interfaces between a random line of unit length on a plane of polish
$N_L^{\alpha\beta}$: numbers of intercepts of α–β interfaces between a random line of unit length on a plane of polish

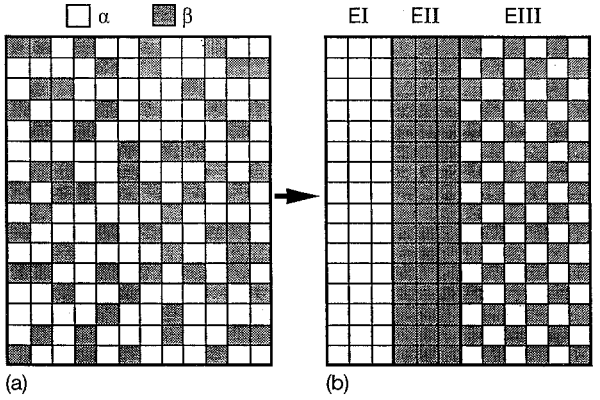

Figure 1 Schematic illustration of the topological transformation from (a) microstructure A to (b) microstructure B. This graph is just a *schematic* illustration of the topological transformation and does not represent any quantitative information such as the volume fraction, grain size and grain shape. The (isotropic) mechanical properties of microstructure A are represented by loading of the equivalent microstructure B in the aligned direction.

only phase boundaries in EIII. The volume fraction of EIII is defined by the degree of separation, F_s, and its grain size is defined by the volume fraction weighted-average grain size, $\bar{d}_{III}$, i.e.

$$\bar{d}_{III} = d_\alpha f_{\alpha III} + d_\beta f_{\beta III} \quad (3)$$

where $f_{\alpha III}$ and $f_{\beta III}$ are the volume fractions of α-phase and β-phase in EIII, respectively. It is obvious that both geometrical and topological parameters in microstructures A (Fig. 1a) and B (Fig. 1b) are identical along the aligned direction. Furthermore, microstructures A and B are mechanically equivalent along the aligned direction of B [15, 17, 18]. As a consequence of this topological transformation, the determination of the mechanical properties of a complicated dual-phase microstructure can be replaced by an analysis of the simpler but equivalent microstructure with three well-defined microstructural elements.

It is necessary to emphasize the following points: (i) Fig. 1 is just a *schematic* illustration of the topological transformation, and does not represent any quantitative information such as the volume fraction, grain size and grain shape; (ii) it is important to make a clear distinction between the different volume fractions. f_α, $f_{\alpha III}$ and $f_{\alpha c}$ represent volume fractions of the α-phase in the composite, of the α-phase in element III and of the continuous α-phase in the 3-E body, respectively; (iii) microstructure B is mechanically equivalent to microstructure A only in the aligned direction (Fig. 1b), which means that the mechanical properties of microstructure A (which is isotropic) can be represented by those of microstructure B (which is anisotropic) in the aligned direction.

3. The total strain distribution among the three microstructural elements

Consider the total strain distribution among the three microstructural elements in the 3-E body at a certain point during the deformation process of an α–β composite when a uniaxial stress σ^A_{33} is applied along the aligned direction (see Fig. 2). In the first case, the elastic constants of all three elements are assumed to

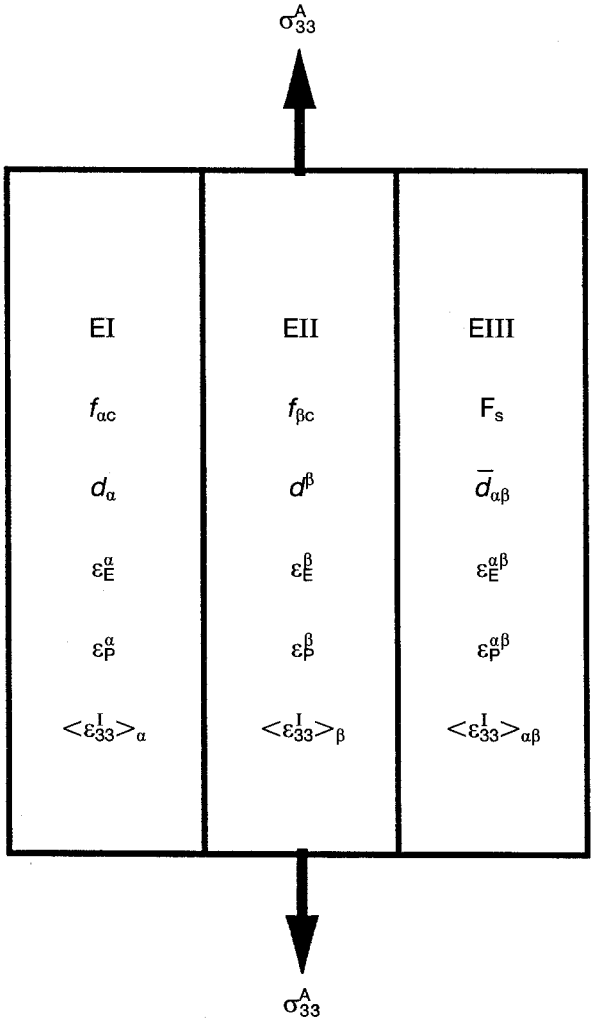

Figure 2 A schematic illustration of the 3-E body under the uniaxially applied stress σ^A_{33}. Also shown here are the microstructural parameters and the various strains in each microstructural element.

be equal. In other words, in this case we are dealing only with elastically homogeneous composites.

Assume that a continuum body consists of two microstructural elements, i and j, which are parallelly aligned, and is subjected to a uniaxial tensile stress. According to Brown and Clarke [19] the mean internal strain field in each element can be described by the following equations

$$\langle \varepsilon^I_{33} \rangle_i = \gamma_{33} f_j (\varepsilon^j_P - \varepsilon^i_P) \quad (4a)$$

$$\langle \varepsilon^I_{33} \rangle_j = \gamma_{33} f_i (\varepsilon^i_P - \varepsilon^j_P) \quad (4b)$$

where $\langle \varepsilon^I_{33} \rangle_i$ and $\langle \varepsilon^I_{33} \rangle_j$ are the mean internal stresses along the tensile direction in the elements i and j, γ_{33} is the strain accommodation tensor [19] along the tensile direction, ε^i_P and ε^j_P are the plastic strains in elements i and j, and f_i and f_j are the volume fractions of elements i and j.

The total strain in elements i and j is the sum of elastic strain, ε_E, the plastic strain, ε_P, and the mean internal strain, $\langle \varepsilon^I_{33} \rangle$, as shown in Fig. 2, i.e.

$$\varepsilon^i_T = \varepsilon^i_E + \varepsilon^i_P + \langle \varepsilon^I_{33} \rangle_i$$
$$= \varepsilon^i_E + \varepsilon^i_P + \gamma_{33} f_j (\varepsilon^j_P - \varepsilon^i_P) \quad (5a)$$

$$\varepsilon^j_T = \varepsilon^j_E + \varepsilon^j_P + \langle \varepsilon^I_{33} \rangle_j$$
$$= \varepsilon^j_E + \varepsilon^j_P + \gamma_{33} f_i (\varepsilon^i_P - \varepsilon^j_P) \quad (5b)$$

The total strain difference between elements i and j is

$$\varepsilon_T^i - \varepsilon_T^j = (\varepsilon_E^i - \varepsilon_E^j) + (\varepsilon_P^i - \varepsilon_P^j) + \gamma_{33}(f_j + f_i)(\varepsilon_P^j - \varepsilon_P^i) = 0 \quad (6)$$

because $f_j + f_i = 1$, $\gamma_{33} = 1$ and $\varepsilon_E^i = \varepsilon_E^j$.
Thus

$$\varepsilon_T^i = \varepsilon_T^j \quad (7)$$

As a consequence of the above derivation, it is easy to obtain the following relation for the 3-E body

$$\varepsilon_T^\alpha = \varepsilon_T^\beta = \varepsilon_T^{\alpha\beta} = \varepsilon_T^c \quad (8)$$

where ε_T^α, ε_T^β, $\varepsilon_T^{\alpha\beta}$ and ε_T^c denote the total strain in Element I, II, III and the whole composite (the 3-E body), respectively.

It is not possible at the moment to derive Equation 8 theoretically in the case of inhomogeneous composites (where the elastic constants of the constituent phases are different). However, Equation 8 will follow from the strain compatibility requirement if the composite is free from debonding [20]. Therefore, Equation 8 should be applicable to both homogeneous and inhomogeneous composites. Furthermore, Equation 8 is a direct consequence of the various interactions in the whole 3-E body [15].

Equation 8 indicates that in the cases of both homogeneous and inhomogeneous composites the total strains along the tensile direction in the three parallelly aligned microstructural elements are the same and equal to the total strain in the whole composite (the 3-E body), if a uniaxial stress is applied along the aligned direction of the three microstructural elements.

4. The generalized law of mixtures

4.1. The *in situ* stress distribution among the three microstructural elements

At a certain deformation point during the deformation process of an α–β composite, the *in situ* total strain in each microstructural element is ε_T^α in EI, ε_T^β in EII and $\varepsilon_T^{\alpha\beta}$ in EIII. Assuming that the 3-E body undergoes a further deformation, $\delta\varepsilon_T^c$, under the applied stress, the plastic strain in each element at this point will be $\varepsilon_T^\alpha + \delta\varepsilon_T^\alpha$ in EI, $\varepsilon_T^\beta + \delta\varepsilon_T^\beta$ in EII and $\varepsilon_T^{\alpha\beta} + \delta\varepsilon_T^{\alpha\beta}$ in EIII. The strain increment must satisfy the virtual work principle. Hence

$$\sigma^c\delta\varepsilon_T^c = \sigma^\alpha\delta\varepsilon_T^\alpha f_{\alpha c} + \sigma^\beta\delta\varepsilon_T^\beta f_{\beta c} + \sigma^{\alpha\beta}\delta\varepsilon_T^{\alpha\beta}F_s \quad (9)$$

where σ^α, σ^β, $\sigma^{\alpha\beta}$ and σ^c denote the *in situ* stresses of Element I, II, III and the whole composite, respectively. Combining Equations 8 and 9, one obtains

$$\sigma^c = \sigma^\alpha f_{\alpha c} + \sigma^\beta f_{\beta c} + \sigma^{\alpha\beta}F_s \quad (10)$$

Equation 10 is therefore the general equation describing the *in situ* stress distribution among the three microstructural elements. Equation 10 has a similar form to the law of mixtures.

4.2. The partition of the *in situ* plastic strain among the three microstructural elements in two-ductile-phase alloys

At a certain point of plastic deformation of two-ductile-phase alloys, the *in situ* plastic strain in each microstructural element is ε_P^α in EI, ε_P^β in EII and $\varepsilon_P^{\alpha\beta}$ in EIII. Assuming that the 3-E body undergoes a further plastic deformation, $\delta\varepsilon_P^c$, the plastic strain in each element at this point will be $\varepsilon_P^\alpha + \delta\varepsilon_P^\alpha$ in EI, $\varepsilon_P^\beta + \delta\varepsilon_P^\beta$ in EII and $\varepsilon_P^{\alpha\beta} + \delta\varepsilon_P^{\alpha\beta}$ in EIII. According to Fan [15] we have the following equation

$$\delta\varepsilon_P^c = f_{\alpha c}\delta\varepsilon_P^\alpha + f_{\beta c}\delta\varepsilon_P^\beta + F_s\delta\varepsilon_P^{\alpha\beta} + \frac{B}{\sigma_{33}^A} \times \left\{ \begin{array}{l} [f_{\beta c}(\varepsilon_P^\beta + \delta\varepsilon_P^\beta) + F_s(\varepsilon_P^{\alpha\beta} + \delta\varepsilon_P^{\alpha\beta}) - (f_{\beta c} + F_s)(\varepsilon_P^\alpha + \delta\varepsilon_P^\alpha)]f_{\alpha c}\delta\varepsilon_P^\alpha \\ + [f_{\alpha c}(\varepsilon_P^\alpha + \delta\varepsilon_P^\alpha) + F_s(\varepsilon_P^{\alpha\beta} + \delta\varepsilon_P^{\alpha\beta}) - (f_{\alpha c} + F_s)(\varepsilon_P^\beta + \delta\varepsilon_P^\beta)]f_{\beta c}\delta\varepsilon_P^\beta \\ + [f_{\alpha c}(\varepsilon_P^\alpha + \delta\varepsilon_P^\alpha) + f_{\beta c}(\varepsilon_P^\beta + \delta\varepsilon_P^\beta) - (f_{\alpha c} + f_{\beta c})(\varepsilon_P^{\alpha\beta} + \delta\varepsilon_P^{\alpha\beta})]F_s\delta\varepsilon_P^{\alpha\beta} \end{array} \right\} \quad (11)$$

where $B = (5 - 4\nu)E/4(1 - \nu^2)$, E is Young's modulus and ν is Poisson's ratio. Equation 11 describes the plastic strain distribution among the three microstructural elements of the whole 3-E body. However, the contribution from the terms in the curved brackets multiplied by B/σ_{33}^A is negligibly small compared with that from the other terms [15]. Therefore, to a very good approximation, the plastic strain distribution among the three microstructural elements can be described by the following equation

$$\delta\varepsilon_P^c = f_{\alpha c}\delta\varepsilon_P^\alpha + f_{\beta c}\delta\varepsilon_P^\beta + F_s\delta\varepsilon_P^{\alpha\beta} \quad (12)$$

Equation 12 has a similar form to the law of mixtures.

4.3. Young's modulus of an α–β composite

If the deformation of an α–β composite is confined within the elastic limit, the *in situ* stress distribution in the three microstructural elements is still described by Equation 10. Dividing both sides of Equation 10 by the *in situ* elastic strain in the whole 3-E body, ε_E^c, and noting that $\varepsilon_E^\alpha = \varepsilon_E^\beta = \varepsilon_E^{\alpha\beta} = \varepsilon_E^c$, we get the following equation

$$\sigma^c/\varepsilon_E^c = (\sigma^\alpha/\varepsilon_E^\alpha)f_{\alpha c} + (\sigma^\beta/\varepsilon_E^\beta)f_{\beta c} + (\sigma^{\alpha\beta}/\varepsilon_E^{\alpha\beta})F_s \quad (13)$$

Then, from Hook's law we have

$$E^c = E^\alpha f_{\alpha c} + E^\beta f_{\beta c} + E^{\alpha\beta}F_s \quad (14)$$

where E^α, E^β, $E^{\alpha\beta}$, and E^c are the Young's moduli of Elements I, II, III and the whole 3-E body, respectively. Equation 14 relates the Young's modulus of an α–β composite to the Young's moduli of the three microstructural elements.

4.4. The yield strength of two-ductile-phase alloys

Fan *et al.* [18] have derived the following equation for two-ductile-phase alloys

$$\sigma_y^c = \sigma_y^\alpha f_{\alpha c} + \sigma_y^\beta f_{\beta c} + \sigma_y^{\alpha\beta} F_s \quad (15)$$

where σ_y^α, σ_y^β, $\sigma_y^{\alpha\beta}$ and σ_y^c denote the yield strength of Elements I, II, III and of the whole composite. Equation 15 is the general expression for the yield strength of two-ductile-phase alloys. By applying the Hall–Petch relation [21, 22] to each microstructural element in Equation 15, we obtain

$$\sigma_y^c = (\sigma_y^{o\alpha} + k_y^\alpha d_\alpha^{-1/2}) f_{\alpha c} + (\sigma_y^{o\beta} + k_y^\beta d_\beta^{-1/2}) f_{\beta c} + (\sigma_y^{o\alpha\beta} + k_y^{\alpha\beta} \bar{d}_{\alpha\beta}^{-1/2}) F_s \quad (16)$$

where σ_y^o is the friction stress and k_y is the Hall–Petch coefficient.

Furthermore, expressions for σ_y^{oc} and k_y^c in two-ductile-phase alloys can also be derived as shown elsewhere [18]

$$\sigma_y^{oc} = \sigma_y^{o\alpha} f_{\alpha c} + \sigma_y^{o\beta} f_{\beta c} + \sigma_y^{o\alpha\beta} F_s \quad (17)$$

$$k_y^c = k_y^\alpha f_{\alpha c} + k_y^\beta f_{\beta c} + k_y^{\alpha\beta} F_s \quad (18)$$

Again, σ_y^c, σ_y^{oc} and k_y^c all have a similar form to the law of mixtures.

4.5. The flow stress of an α–β composite

In the case of plastic deformation of an α–β composite, the following equation can be obtained from Equation 10

$$\sigma_f^c = \sigma_f^\alpha f_{\alpha c} + \sigma_f^\beta f_{\beta c} + \sigma_f^{\alpha\beta} F_s \quad (19)$$

where σ_f^α, σ_f^β, $\sigma_f^{\alpha\beta}$ and σ_f^c are the *in situ* flow stresses in Elements I, II, III and of the whole 3-E body, respectively. Equation 19 also has a similar form to the law of mixtures.

4.6. The generalized law of mixtures

The mechanical properties of an α–β composite are here denoted by P^c, where P^c represents the Young's modulus, E^c, the yield strength, σ_y^c, the flow stress, σ_f^c, the friction stress, σ_y^{oc}, and the overall Hall–Petch coefficient, k_y^c. If the mechanical properties of EI, EII and EIII in the 3-E body are denoted P^α, P^β and $P^{\alpha\beta}$, respectively, P^c can then be expressed as the sum of the relative contributions from each microstructural element, according to the previous analysis, i.e.

$$P^c = P^\alpha f_{\alpha c} + P^\beta f_{\beta c} + P^{\alpha\beta} F_s \quad (20)$$

Equation 20 is called here the generalized law of mixtures, and can be used to predict a number of mechanical properties of two-phase composites with any volume fraction, grain shape and phase distribution.

Now, let us apply the concept of directional contiguity [15] to a composite reinforced with perfectly aligned continuous fibres along the aligned direction. In this case, $F_s = 0, f_{\alpha c} = f_\alpha$ and $f_{\beta c} = f_\beta$ and the generalized law of mixtures (Equation 20) reduces to the classical linear law of mixtures, i.e.

$$P^c = P^\alpha f_\alpha + P^\beta f_\beta \quad (21)$$

Therefore, the classical linear law of mixtures is a specific case of the generalized law of mixtures. However, in contrast to the classical linear law of mixtures (Equation 21), the generalized law of mixtures (Equation 20): (i) can take into account the various interactions, especially the interactions between the particles of the same phase in a random phase mixture [15]; (ii) is applicable not only to continuous fibre composites but also to particulate systems with any volume fraction, grain shape and phase distribution; (iii) can be derived from continuum mechanics; (iv) can be applied to predict a variety of mechanical properties, such as Young's modulus, yield strength, flow stress, the overall friction stress, σ_y^{oc}, and the overall Hall–Petch coefficient, k_y^c.

5. Applications of the generalized law of mixtures

5.1. Prediction of Young's modulus of continuous fibre and particulate composites

Below, the generalized law of mixtures will be applied to the continuous tungsten fibre-reinforced copper matrix composites, the Co/WC_p, the Al/SiC_p composites and glass-filled epoxy composites to predict their Young's moduli. The theoretical predictions will be compared with experimental data drawn from the literature and with the predictions of other theories.

The Young's moduli of copper and tungsten were calculated from the experimental results of Foreman [23] ($\mu_{Cu} = 42$ GPa and $\nu_{Cu} = 0.45$) and Lowrie and Gonas [24] ($\mu_w = 162$ GPa and $\nu_w = 0.28$), respectively. The elastic constants and Poisson's ratios of cobalt and WC were taken from the experimental results of Paul [25] and Doi *et al.* [26]. The mechanical properties of aluminium and SiC were adopted from the works of Withers [27] and Davis [28]. The elastic constants and Poisson's ratios of epoxy and glass beads used for this calculation were the same as those used by Ahmed and Jones [29]. The mechanical properties of the constituent phases in the four composite systems concerned here are summarized in Table II.

In the case of continuous tungsten fibre-reinforced copper composite, $F_s = 0$, $f_{\alpha c} = f_\alpha$ and $f_{\beta c} = f_\beta$. The

TABLE II The mechanical properties of constituent phases used for prediction of Young's moduli

System	Phase	G (GPa)	E (GPa)	ν
Cu/W_f [23, 24]	Cu	42	121.8	0.45
	W	162	414.7	0.28
Co/WC_p [25, 26]	Co	80.2	210.0	0.31
	WC	293.1	700.0	0.194
Al/SiC_p [27, 28]	Al	26.1	70.0	0.34
	SiC	189.0	420.7	0.19
Glass-filled epoxy [29]	Glass beads	28.7	70.0	0.22
	Epoxy	1.33	3.7	0.39

predicted Young's moduli for this system are compared in Fig. 3 with the experimental results of McDanels *et al.* [30]. Fig. 3 shows that there is a very good agreement between the predictions by the generalized law of mixtures and the experimental results [30].

In many investigations of the mechanical properties of two-phase materials, the Co/WC_p composites have been used as a model system for which numerous experimentally measured E values are available in the literature. A further reason for the choice of this system is that the topological parameters required for the calculation can be found in the experimental work of Fischmeister and Exner [31] and Lee and Gurland [9]. Their contiguity data for the WC phase (denoted as the β-phase) in Co–WC composites can be expressed as

$$C_\beta = f_\beta^3 \tag{22}$$

Here it is assumed that the contiguity of cobalt (denoted the α-phase) follows the same trend of variation with the volume fraction of the cobalt phase, i.e.

$$C_\alpha = f_\alpha^3 \tag{23}$$

The other required parameters can be calculated from the following equations [15]

$$f_{\alpha c} = C_\alpha f_\alpha = f_\alpha^4 \tag{24}$$

$$f_{\beta c} = C_\beta f_\beta = f_\beta^4 \tag{25}$$

$$F_s = 1 - f_{\alpha c} - f_{\beta c} \tag{26}$$

$$f_{\alpha III} = \frac{f_\alpha - f_{\alpha c}}{F_s} \tag{27}$$

$$f_{\beta III} = \frac{f_\beta - f_{\beta c}}{F_s} \tag{28}$$

In general, the continuous volumes of α- and β-phases are assumed to be given by the following equations

$$f_{\alpha c} = f_\alpha^m \tag{29}$$

$$f_{\beta c} = f_\beta^n \tag{30}$$

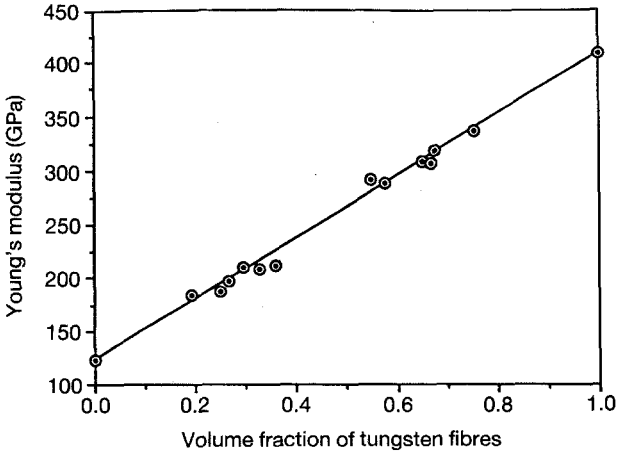

Figure 3 A comparison of (——) the predicted Young's moduli of continuous Cu–W composites and (⊙) the experimental results of McDanels *et al.* [30].

The Young's moduli of the Co–WC_p system calculated by the generalized law of mixtures are shown in Fig. 4 as a function of the volume fraction of the WC phase. Also shown in Fig. 4 are the experimental data from a number of investigators [26, 32–35], the results from finite element method (FEM) calculations [36] and the theoretical predictions by Hashin–Shtrikman (H–S) lower and upper bounds [32]. Fig. 5 shows the high volume fraction region in Fig. 4. In Figs 4 and 5 the theoretical predictions of the present approach are well within the H–S lower and upper bounds. Furthermore, there is a better agreement between the predictions by the generalized law of mixtures and the experimental results especially at high volume fractions of the WC phase (Fig. 5) than the theoretical predictions of the H–S bounds.

In recent years there has been a great deal of interest in the Al/SiC_p composites and experimental data on the Young's modulus is available. Therefore, it would

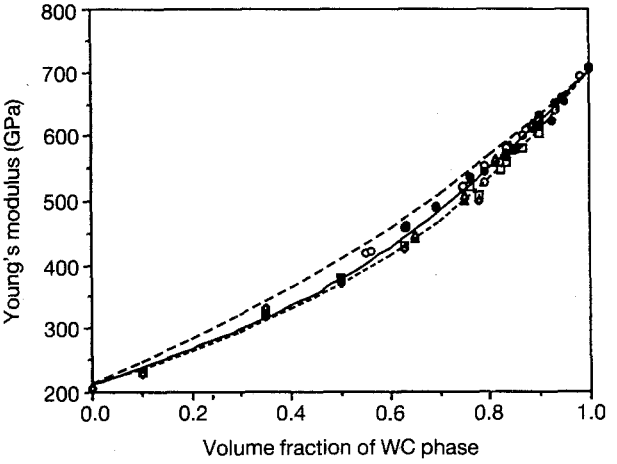

Figure 4 A comparison of the theoretically predicted Young's moduli of the Co-WC_p system by the present approach (——) with the theoretical predictions by H–S upper (– – –) and lower (- - -) bounds [32], the experimental results (○) [26], (⊡) [32], (◇) [33], (□) [34], (●) [35], and calculations using finite element method (▲, △) [36].

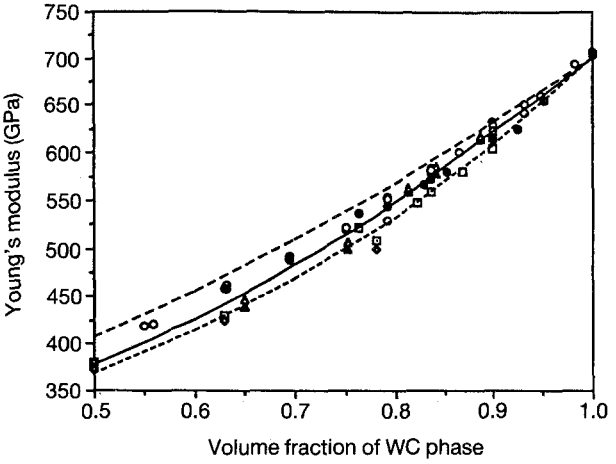

Figure 5 A comparison at high volume fractions of WC particles of the theoretically predicted Young's moduli of the Co-WC_p system by the present approach (——) with the theoretical predictions by H–S upper (– – –) and lower (- - -) bounds [32], the experimental results (○) [26], (⊡) [32], (◇) [33], (□) [34], (●) [35], and calculations using finite element method (▲, △) [36].

be very interesting to apply the generalized law of mixtures to Al/SiC_p composites. Because the topological parameters required for the calculation are not available for the Al/SiC_p system, it will be assumed that, as in the Co–WC system, the continuous volumes of the α- and β-phases are represented by f_α^4 and f_β^4, respectively, i.e. $m = n = 4$ in Equations 29 and 30. The other required topological parameters can be calculated from Equations 26–28.

A comparison of the Young's moduli of Al/SiC_p composites is made in Fig. 6 from the theoretical predictions by the generalized law of mixtures, the H–S bounds and the recently reported experimental results [37–42]. The small variations in the Young's moduli of the different unreinforced aluminium alloys have not been considered in this comparison. Fig. 6 indicates that the theoretical predictions by the generalized law of mixtures are in a better agreement with the experimental results than those by H–S bounds.

Another group of composites of commercial interests are the polymer matrix composites, where the stiffness ratio of the two constituent phases is normally large. In a glass-filled epoxy composite E_β/E_α can be as large as 20. Therefore, from both the theoretical and practical point of view, it is interesting to apply the generalized law of mixtures to this system. The required topological parameters are assumed to follow Equations 24–28.

The predicted Young's moduli for graded glass beads-filled epoxy composites as a function of volume fraction of glass beads are shown in Fig. 7 and compared with the experimental data reported elsewhere [43, 44], as well as with the theoretical predictions by the H–S bounds [32]. Fig. 7 indicates that the H–S lower bound is closer to the experimental data than the predictions by the present approach under the above microstructural condition. However, as we know, in the graded glass bead-filled epoxy system the filler normally tends to be much more separated than the matrix. Thus, if the continuous volume of the glass beads is assumed to be 0 ($f_{\beta c} = 0$) and that of the α-phase to be $f_{\alpha c} = f_\alpha^3 (m = 3)$, the calculated Young's moduli of this system are much closer to the experimental data.

Furthermore, as shown in Figs 4–7, the Young's moduli of particulate composites predicted by the generalized law of mixtures are close to the H–S lower bound at low volume fractions and approaching the H–S upper bound at high volume fraction. This is an interesting result, because one would intuitively expect the lower bound to be more closely followed at low volume fractions, whereas the stiffness could approach the upper bound at high volume fractions, as pointed out by Withers *et al.* [45].

5.2. Prediction of the yield strength and flow stress of two-phase composites

Equations 15 and 19 have been applied to copper-matrix composites reinforced with continuous tungsten fibres to predict the yield strength and the flow stress of this system. The calculated yield strengths and flow stresses are shown in Figs 8 and 9,

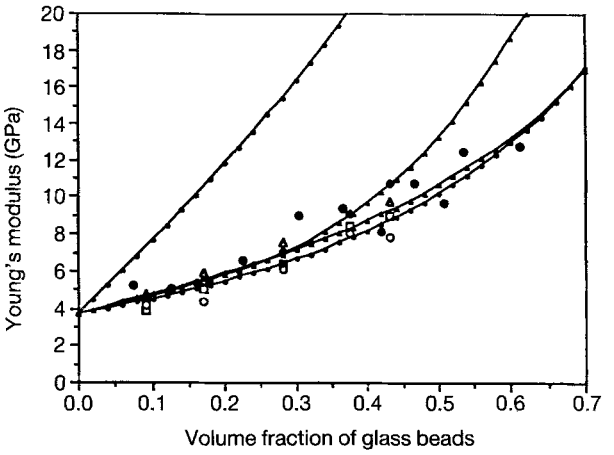

Figure 7 A comparison at low volume fraction of glass beads of the theoretically predicted Young's moduli of glass-filled epoxy composites by the present approach with (▲) $m = n = 4$ and (△) $f\beta_c = 0$ and $m = 3$, the theoretical predictions by H–S upper (◆) and lower (○) bounds [30] and experimental results (□, ◇, ○, △) [43], (●) [44].

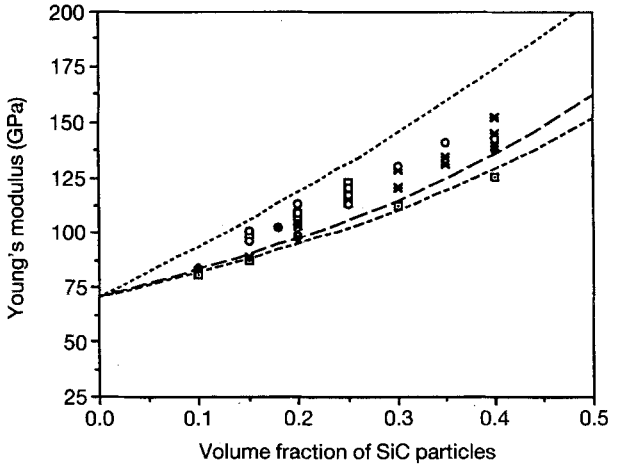

Figure 6 A comparison at low volume fraction of SiC particles of the theoretically predicted Young's moduli of Al/SiC_p composites by the present approach (———), the theoretical predictions by H–S upper (– – –) and lower (- - -) bounds [32] and experimental results (⊡) [37], (◇) [38], (*) [39], (□) [40], (●) [41], (○) [42].

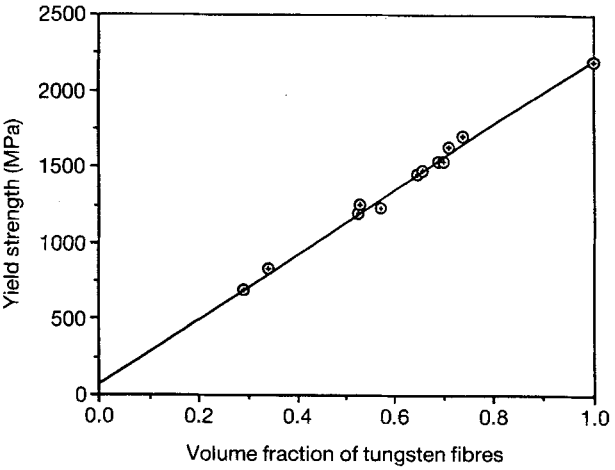

Figure 8 A comparison between the predicted yield strengths (—) of Cu–W composites and the experimental results (⊕) of McDanels *et al.* [30].

respectively, and compared with the corresponding experimental results of McDanels *et al.* [30]. There is a very good agreement between the predictions and the experimental results.

Fan [15] has developed an approach for the calculation of the true stress–true strain curve of the EIII body in two-ductile-phase alloys. If the yield strength is defined as the flow stress at 0.2% plastic strain, the yield strength of EIII can be evaluated from the calculated flow curve of the EIII body. Therefore, Equation 15 can be applied to predict the yield strength of two-ductile-phase alloys. The predicted yield strengths of α–β Ti–Mn alloys are presented in Fig. 10 and compared with the predictions of the classical linear law of mixtures and the experimental results of Margolin and co-workers [46, 47]. Fig. 10 indicates that there is good agreement between the predictions by the generalized law of mixtures and the experimental results.

The same approach [15] has been applied to calculate the flow curve of the EIII body in a ferrite–martensite dual-phase steel with 50% martensite phase. The calculated results are presented in Fig. 11 together with the prescribed flow curves of the ferrite-phase (EI) and martensite phase (EII) [13]. From these the flow curve of this dual-phase steel can be constructed according to Equation 19, and is shown in Fig. 11. The topological parameters used in this calculation are from the experimental data of Uggowitzer and Stuwe [48]. Similar results for two Ti–Mn alloys with 82.3% and 16.4% α-phase are presented in Fig. 12 and compared with the experimental results of Ankem and Margolin [46]. Figs 11 and 12 indicate that there is a good agreement between the predictions by the generalized law of mixtures and the experimental results.

5.3. Predictions of the Hall–Petch constants for Cu–Zn alloys

Fan *et al.* [18] have extended the Hall–Petch relation [21, 22] developed originally for the single-phase

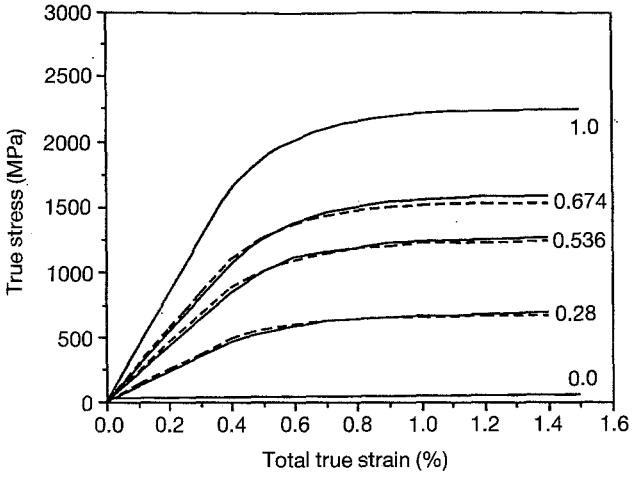

Figure 9 A comparison between the predicted flow curves (– – –) of Cu–W composite and the experimental results (——) of McDanels *et al.* [30]. The given data indicate the volume fractions of tungsten fibres.

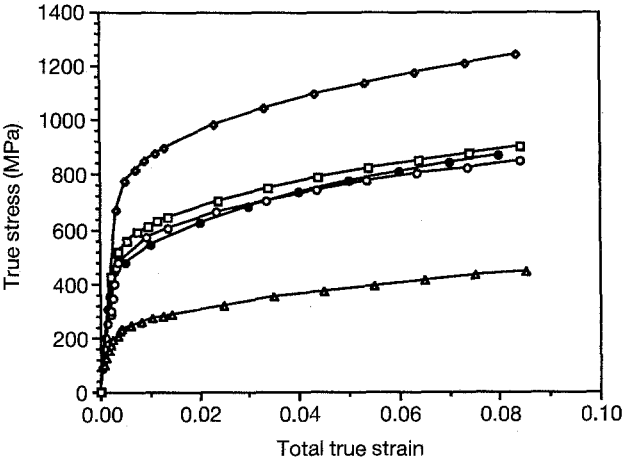

Figure 11 A comparison between the predicted (○) flow curve of a ferrite-martensite dual-phase steel with 50% martensite phase with the corresponding experimental (●) results of Uggowitzer and Stuwe [48]. (▲) EI, (◆) EII, (□) EIII.

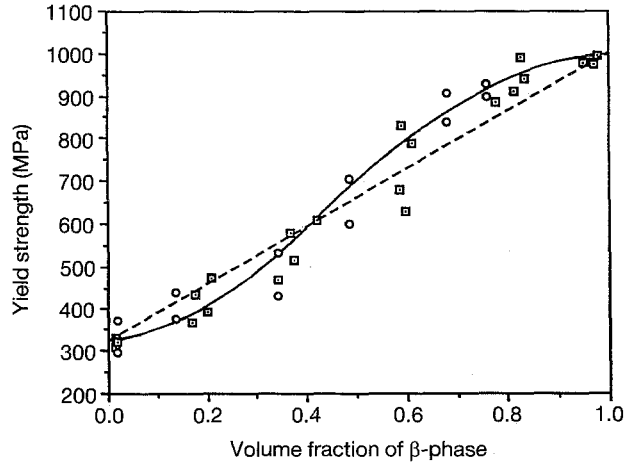

Figure 10 The calculated yield strength of α–β Ti–Mn alloys (——) as a function of volume fraction of the β-phase in comparison with the predictions by the classical linear law of mixtures (– – –) and the experimental results of Margolin and co-workers (⊡) [46], (○) [47].

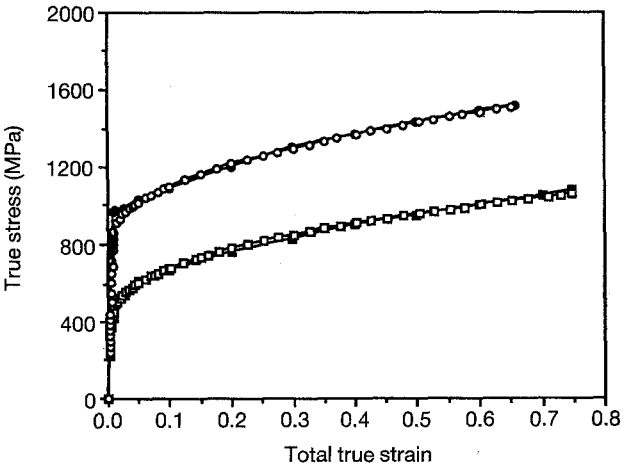

Figure 12 A comparison between the predicted (□, ○) flow curves of two α–β Ti–Mn alloys with different volume fraction of α-phase with the corresponding experimental results (■, ●) of Ankem and Margolin [46]. (■) 0.823, (□) 0.823, (●) 0.164, (○) 0.164.

alloys to two-ductile-phase alloys, and they have applied the extended Hall–Petch relation to α–β Cu–Zn alloys, α–β Ti–Mn alloys and α–γ Fe–Cr–Ni stainless steels. Their results for the Hall–Petch constants in the α–β Cu–Zn system are summarized in Table III.

Using Equations 17 and 18 together with the parameters in Table III, as well as the topological parameters from Werner and Stuwe [49], the overall friction stresses, σ_y^{oc}, and the overall Hall–Petch coefficients, k_y^c, can be calculated. These results are shown in Figs 13 and 14 for σ_y^{oc} and k_y^c, respectively. Figs 13 and 14 show that the theoretical predictions of σ_y^{oc} and k_y^c using the generalized law of mixtures are in good agreement with the data evaluated by Fan *et al.* [18] from the experimental results of Werner and Stuwe [49].

TABLE III Summary of the Hall–Petch constants in the α–β Cu–Zn system from [18]

Element	σ_y^o(MPa)	k_y (MPa mm$^{1/2}$)
EI	35	11.4
EII	75	11.9
EIII	$\sigma_y^{o\alpha} f_\alpha + \sigma_y^{o\beta} f_\beta$	14.5

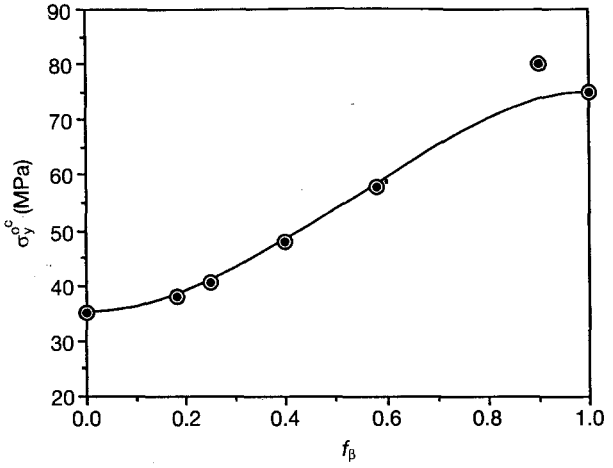

Figure 13 A comparison between the predicted (——) overall friction stresses in Cu–Zn alloys with the results (⊙) evaluated by Fan *et al.* [18] from the experimental data of Werner and Stuwe [49].

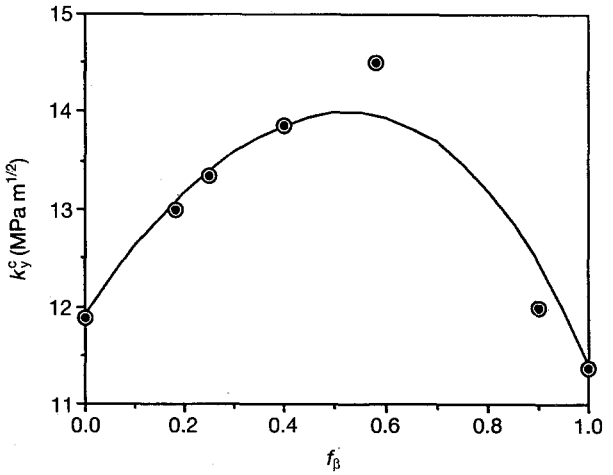

Figure 14 A comparison between the theoretical predictions (——) of the overall Hall–Petch coefficients in Cu–Zn alloys with the results (⊙) evaluated by Fan *et al.* [18] from the experimental data of Werner and Stuwe [49].

6. Conclusion

A generalized law of mixtures has been derived theoretically for the prediction of the mechanical properties of two-phase composites. In contrast to the classical linear law of mixtures, which is empirical and requires some explicit assumptions, the generalized law of mixtures can be derived from continuum mechanics. It has been shown that the classical linear law of mixtures is a specific case of the generalized law of mixtures. The generalized law of mixtures is applicable to two-phase composites with any volume fraction, grain shape and phase distribution and can predict a variety of mechanical properties. There is an excellent agreement between the predictions of the generalized law of mixtures and the experimental results drawn from the literature.

Acknowledgements

The authors thank Professor J. E. Castle for the provision of laboratory facilities and Dr P. A. Smith for useful discussions. One of us (Z.F.) also acknowledges the financial support by the Procurement Executive of the Ministry of Defence, UK.

References

1. W. VOIGHT, *Wied. Ann.* **38** (1889) 573.
2. I. TAMURA, Y. TOMOTA and H. OZAWA, in "Proceedings of the 3rd International Conference on Strength of Metals and Alloys", Vol. 1 (Institute of Metals, and Iron and Steel Institute, London, 1973) p. 611.
3. H. FISCHMEISTER and B. KARLSON, *Z. Metallkde* **68** (1977) 311.
4. P. D. FUNKENBUSCH, J. K. LEE and T. H. COURTNEY, *Met. Trans.* **18A** (1987) 1249.
5. Y. L. SU and J. GURLAND, *Mater. Sci. Eng.* **95** (1987) 151.
6. S. ANKEM and H. MARGOLIN, *Met. Trans.* **13A** (1982) 595.
7. N. C. GEOL, S. SANGAL and K. TANGRI, *ibid.* **16A** (1985) 2013.
8. *Idem, ibid.* **16A** (1985) 2023.
9. H. C. LEE and J. GURLAND, *Mater. Sci. Eng.* **33** (1978) 125.
10. S. ANKEM and H. MARGOLIN, *Met. Trans.* **13A** (1982) 603.
11. B. KARLSON and G. LINDEN, *Mater. Sci. Eng.* **17** (1975) 209.
12. J. GURLAND and K. CHO, in "Proceedings of the 7th International Symposium on Stereology", Vol. 6, Caen, France, 1987, edited by J. L. Chermant (Acta Stereology, Ljubliana, Yugoslavia, 1987) Suppl. III, p. 135.
13. K. CHO and J. GURLAND, *Met. Trans.* **19A** (1988) 2027.
14. J. GURLAND, *Trans. Met. Soc. AIME* **212** (1958) 452.
15. Z. FAN, PhD Thesis, University of Surrey (1993).
16. E. E. UNDERWOOD, in "Stereology and Quantitative Metallography", ASTM STP 504 (American Society for Testing and Materials, Philadelphia, PA, 1972) p. 3.
17. Z. FAN, P. TSAKIROPOULOS and A. P. MIODOWNIK, *Mater. Sci. Technol.* **8** (1992) 922.
18. Z. FAN, P. TSAKIROPOULOS, P. A. SMITH and A. P. MIODOWNIK, *Philos. Mag.* **67A** (1993) 515.
19. L. M. BROWN and D. R. CLARKE, *Acta Metall.* **23** (1975) 821.
20. H. FORD, "Advanced Mechanics of Materials" (Wiley, New York, 1963) pp. 115–21, 129–31.
21. E. O. HALL, *Proc. Phys. Soc. Lond.* **B64** (1951) 747.

22. N. J. PETCH, *J. Iron Steel Inst.* **174** (1953) 25.
23. A. J. E. FOREMAN, *Acta Metall.* **3** (1955) 322.
24. R. LOWRIE and A. M. GONAS, *J. Appl. Phys.* **36** (1965) 2189.
25. B. PAUL, *Trans TMS-AIME* **218** (1960) 36.
26. H. DOI, Y. FUJIWARA, K. MIYAKE and Y. OSAWA, *Met. Trans.* **1** (1970) 147.
27. P. J. WITHERS, PhD thesis, University of Cambridge (1988).
28. L. C. DAVIS, *Metall. Trans.* **22A** (1991) 3065.
29. S. AHMED and F. R. JONES, *J. Mater. Sci.* **25** (1990) 4933.
30. D. L. McDANELS, R. W. JECH and J. W. WEETON, *Trans. Met. Soc. AIME* **233** (1965) 636.
31. H. FISCHMEISTER and H. E. EXNER, *Arch. Eisenhuttenw.* **37** (1966) 499.
32. Z. HASHIN and S. SHTRIKMAN, *J. Mech. Phys. Solids* **11** (1963) 127.
33. C. NISHIMATSU and J. GURLAND, *Trans. ASM* **52** (1960) 469.
34. B. O. JAENSSON and B. O. SUNDSTROM, *Mater. Sci. Eng.* **9** (1972) 217.
35. F. F. VORONOV and D. B. BALASHOV, *Phys. Metals Metallogr.* **2** (1960) 127.
36. R. KEIFFER and P. SCHWARZKOPF, in "Hartstoffe und Harmetalle" (Springer, Vienna, 1953).
37. D. L. McDANELS, *Metall. Trans.* **16A** (1985) 1105.
38. M. W. MAHONEY, A. K. GHOSH and C. C. BAMPTON, in "Proceedings of ICCM VI/ECCM2", Vol. 2, edited by F. L. Mathews *et al.* (Elsevier, London, 1987) p. 272.
39. DWA Composite Specialities Inc., "Guide to Composite Materials" (ASM, 1987).
40. R. L. TRUMPER, *Metal Mater.* (November) (1987) 31662.
41. W. C. HARRIGAN Jr, *J. Metals* (August) (1991) 4332.
42. A. L. GEIGER and J. A. WALKER, *ibid* August (1991) 8.
43. S. SPANOUDAKIS and R. J. YOUNG, *J. Mater. Sci.* **19** (1984) 487.
44. S. AHMED and F. R. JONES, *Composites* **21** (1990) 81.
45. P. J. WITHERS, W. M. STOBBS and O. B. PEDERSEN, *Acta Metall.* **37** (1989) 3061.
46. S. ANKEM and H. MARGOLIN, *Met. Trans.* **17A** (1986) 2209.
47. J. S. PARK and H. MARGOLIN, *ibid.* **15A** (1984) 155.
48. P. UGGOWITZER and H. P. STUWE, *Z. Metallkde* **73** (1982) 277.
49. E. WERNER and H. P. STUWE, *Mater. Sci. Eng.* **68** (1984–1985) 175.

Received 2 October 1992
and accepted 8 June 1993